Engineering in Life Sciences

Eng. Life Sci. **2018**, *18*, 732–742 www.els-journal.com

Elham Vatankhah

Department of Bio-systems, Faculty of New Technologies Engineering, Shahid Beheshti University, Tehran, Iran

Research Article

Rosmarinic acid-loaded electrospun nanofibers: In vitro release kinetic study and bioactivity assessment

This study seeks to develop a nanofibrous matrix containing rosmarinic acid (RosA), an herbal non-steroidal anti-inflammatory and antioxidant drug with low water solubility, for drug delivery applications. Neat and two types of RosA-loaded cellulose acetate (CA) mats varying in the initial content of RosA were electrospun. Microstructure of nanofibers, chemistry and physical state of RosA in nanofibers, RosA loading efficiency and RosA release in acetate buffer were investigated. To evaluate bioactivity of RosA-loaded nanofibers, their ability to inhibit protein denaturation was assayed as an indicator of anti-inflammatory properties and their antioxidant activity was determined by radical scavenging assay. The indirect cytotoxicity assay was used to find if there is a cytotoxic response to nanofibers. The homogeneous distribution of the drug within nanofibers through electrospinning led to high loading efficiency, low burst release and prolonged release of a large percentage of RosA over a period of 64h following Fickian diffusion mechanism. Nanofibers with higher RosA content exhibited anti-inflammatory activity comparable to ibuprofen, and higher antioxidant activity compared to nanofibers with lower RosA content. Additionally, extracts from nanofibers did not give any major harmful effect on cells. Sustained release of RosA, and bioactivity of RosA-loaded nanofibers confirmed the potential of the produced matrix as a drug delivery system.

Keywords: Antioxidant activity / Cellulose acetate / Drug delivery system / Electrospun nanofibers / Rosmarinic acid

Additional supporting information may be found online in the Supporting Information section at the end of the article.

Received: March 2, 2018; *revised:* July 9, 2018; *accepted:* September 5, 2018

DOI: 10.1002/elsc.201800046

1 Introduction

A transdermal drug delivery system (TDDS), also known as a patch is designed to deliver a therapeutically effective dose of a drug through the skin into the systemic circulation non-invasively [1] resulting in improvement in bioavailability by avoiding first-pass hepatic metabolism and enzymatic or pH-associated deactivation and flexibility in terminating drug administration by patch removal [2]. An ideal drug candidate for loading in a TDDS would have a molecular weight up to a few hundred Daltons, and affinity for both lipophilic and hydrophilic phases [2]. Transdermal patches containing non-steroidal anti-inflammatory drugs (NSAIDs) are available for management of chronic pains. Among a variety of phytochemicals, polyphenolic phytochemicals have been shown experimentally to inhibit inflammation. Rosmarinic acid (RosA) is a phenolic phytochemical commonly found in many species of the *Boraginaceae* family and the subfamily *Nepetoideae* of the *Lamiaceae* such as rosemary, sage, and mint [3] which exhibits beneficial biological activities including antioxidant, anti- inflammatory, antiviral, and antibacterial properties [4]. Rosmarinic acid with a molecular weight of 360.318 g/mol is classified as a NSAID in chEBI database of the European Bioinformatics Institute (EMBL-EBI).

Correspondence: Dr. Elham Vatankhah (e_vatankhah@sbu.ac.ir), Department of Bio-systems, Faculty of New Technologies Engineering, Shahid Beheshti University, Tehran, Iran

Abbreviations: BSA, bovine serum albumin; **CA**, cellulose acetate; **COX**, cyclooxygenase; **DPPH**, 1,1′-diphenyl-2-picrylhydrazyl; **DSC**, differential scanning calorimetry; **FTIR**, Fourier transform infrared; **MTT**, 3-[4,5-dimethylthiazole-2-yl]-2,5-diphenyltetrazolium bromide; **NF- κB**, nuclear factor-κB; **NSAID**, non-steroidal anti-inflammatory drug; **PBS**, phosphate buffer saline; **RosA**, rosmarinic acid; **SFM**, serum-free medium; **TDDS**, transdermal drug delivery system

It is slightly soluble in water while it is soluble in most organic solvents to approximately 25 mg/mL. The low water solubility and chemical instability of RosA limit its application in pharmaceutical formulations. Encapsulation technologies to design delivery systems are used to improve the solubility, long-term stability and sustained releases of bioactive molecules [5]. To the best of our knowledge, there is lack of information on encapsulation of RosA in nanofibers. In this study, we aimed at development of a cellulose acetate (CA) nanofibrous mat as a carrier for delivery of RosA in order to treat injuries associated to inflammation and investigate whether RosA-loaded CA nanofibers are able to exhibit bioactivities of free RosA including anti-infammatory and antioxidant properties. The electrospun CA nanofibrous mat was chosen due to its capability to support a gradual and monotonous increase in the cumulative release of the drug over the time and limit the initial burst release of the drug [6]. Cellulose- based materials are widely used in the biopharmaceutical processing industry [7], among which electrospun CA mats have been widely used as carriers for topical/ transdermal delivery of NSAIDs [6–11].

2 Materials and methods

2.1 Electrospinning of neat and RosA-loaded nanofibrous mats

Optimizing the solution concentration and electrospinning conditions was the major step towards the preparation of neat and RosA-loaded nanofibers. Finally, CA powder (Sigma Aldrich, Mn ~30 000, acetyl content ~39.8 wt%) was dissolved in 2:1 v/v acetone (Merck)/ Dimetylacetamide (DMAc, Merck) to obtain neat CA solution at a concentration of 12% w/v. Neat CA solution was kept stirring for 5 h. RosA-loaded solutions were prepared by addition of RosA (Sigma Aldrich, 5 wt% or 10 wt% with respect to the polymer) to the neat solution one hour before electrospinning.

The solutions were individually transferred to 1 mL syringe attached to the perfusion pump to adjust the flow rate to 250 μL/h. A high voltage of 20 kV was applied between the needle and the collector covered with aluminum foil to draw the fibers from the spinneret (20 G needle) to the collector. A rotating cylindrical drum set at a speed of 200 rpm was used for collecting nanofibers and a distance of approximately 12 cm was maintained between the spinneret and the collector. Subsequently, the nanofibrous mats including neat CA, CA/5% RosA, and CA/10% RosA nanofibers were vacuum dried to remove any residual solvent and used for further experiments.

2.2 Characterization of neat and RosA-loaded CA nanofibrous mats

The electrospun nanofibers were sputter-coated with gold and visualized using scanning electron microscopy (SEM, Hitachi, SU3500) at an accelerating voltage of 15 kV. The average diameter of each fibrous mat was calculated from 100 random points chosen from at least three different respective SEM micrographs using image analysis software (ImageJ, National Institutes of Health).

Fourier transform infrared (FTIR, Bomem, B-102) analysis over a range of 400–4000 cm^{-1} at a resolution of 4 cm^{-1} was used to investigate the functional groups of RosA powder, CA nanofibers and RosA-loaded CA nanofibers.

The nature of drug and polymer in electrospun neat CA, CA/5% RosA, and CA/10% RosA nanofibers was studied by differential scanning calorimetry (DSC, Mettler Toledo). Thermal properties of the free RosA were also assayed. Samples weighing 4–5 mg each was sealed in aluminum crucibles with lids. Experiments were carried out at a heating rate of 10 K/min in a temperature range of 50–300°C under nitrogen atmosphere.

Sodium acetate buffer solution was used for further studies to simulate the human skin pH of 5.5. To prepare 200 mL of 10 mM acetate buffer solution (pH 5.5), 8.5 mL of 0.2 M aqueous sodium acetate (Sigma Aldrich) solution and 1.5 mL of 0.2 M glacial acetic acid (Merck) were mixed and the volume was made up to 200 mL using distilled water.

The weight loss and swelling behavior of both the neat and RosA-loaded CA nanofibrous mats submersed in sodium acetate buffer solution (pH 5.5) at 37°C for 24 h were calculated using the following equations, respectively ($n = 3$ per group) [12].

$$\text{Weight loss}\,(\%) = \frac{M_i - M_d}{M_i} \times 100$$

$$\text{Degree of swelling}\,(\%) = \frac{M - M_d}{M_d} \times 100$$

where M_i is the initial weight of the sample in its dry state, M_d is the weight of the sample after submersion in the buffer solution in its dry state, and M is the weight of each sample after submersion in the buffer solution for 24 h.

2.3 Drug loading efficiency

To determine the loading efficiency, 5 mg of each specimen was dissolved in 1 mL of acetone. Then, 0.5 mL of the solution was added into 4.5 mL of phosphate buffer saline (PBS, Sigma Aldrich) solution (pH 7.4) and the mixture was centrifuged. The supernatant was used to determine the loading efficiency using a Jenway 6300 spectrophotometer at the wavelength of 325 nm ($n = 3$ per group). The actual amount of RosA loaded in the fibers was interpolated from the calibration curve of RosA in the same solution. Neat CA mats were also considered and their influence on the absorbance was subtracted. The loading efficiency was calculated as:

$$\text{Loading efficiency}\,(\%) = \frac{\text{Actual amount of drug loaded in the mat}}{\text{Initial amount of drug loaded in the solution}} \times 100$$

2.4 In vitro RosA release assay

In order to assess the RosA release from nanofibrous mats, about 5 mg of each sample was submerged in 2 mL of sodium acetate buffer solution (pH 5.5) and placed in a shaking incubator at 37°C and 50 rpm ($n = 3$ per group). At predetermined

time points, the nanofibrous sample was taken out from the buffer and put in another fresh buffer solution. The amount of drug released from the fibers was determined by conversion of the absorbance of RosA in buffer solution read using a Jenway 6300 spectrophotometer at the wavelength of 365 nm to the RosA concentration according to the calibration curve of RosA in the same buffer drawn at the concentrations ranging from 4 to 250 μg/mL. Neat CA mats were also considered and their influence on the absorbance was subtracted. Finally, cumulative absolute amount of RosA released was presented as a function of time. The following equation was also used to calculate the cumulative percentage of RosA released from electrospun nanofibers.

$$\text{Cumulative release (\%)} = \frac{M_t}{M_\infty} \times 100$$

where M_t is the amount of RosA released at time t and M_∞ is the actual amount of RosA loaded in the nanofibrous mats.

The drug release mechanism was also modeled using Ritger-Peppas equation (DDsolver program [13]).

$$\frac{M_t}{M_\infty} = Kt^n$$

Where M_t / M_∞ denotes the drug fraction released at time t, K is a kinetic constant which depends on the physical characteristics of the matrix/ drug system and n is the diffusional exponent indicating the release mechanism [14]. For $n \leq 0.45$, the drug release follows a Fickian diffusion mechanism while for $0.45 > n > 0.89$, the release mechanism obeys a non-Fickian diffusion in which drug released through a combination of the diffusion from the polymeric matrix and the surface erosion of the fibers [15,16].

2.5 In vitro anti-inflammatory assay

Inhibition of protein denaturation evaluated by the method of Mizushima and Kobayashi [17] was used to investigate the anti-inflammatory activity of neat and RosA-loaded CA nanofibers as well as extracts from neat and RosA-loaded nanofibers. First, the calibration curves and concentrations that are expected to exhibit 50% inhibition (IC_{50}) were determined for RosA in both acetone and sodium acetate buffer solution as well as ibuprofen (Alborz Bulk Pharmaceutical Co., Iran), as a standard anti-inflammatory drug in acetone. According to calculated IC_{50} values, test solutions of nanofibers were prepared as described in Supporting Information. Then, 30 μL of each test solution was diluted in 720 μL of PBS solution (pH 7.4). The supernatant of the mixture was added to 750 μL of 3% w/v bovine serum albumin (BSA, Sigma Aldrich) solution (pH 6.8) and incubated at 25 ± 2°C for 15 min. Denaturation was induced by heating the mixture at 60 ± 3°C in a water bath for 10 min. After cooling the samples down to room temperature, turbidity was measured spectrophotometrically using a Jenway 6300 spectrophotometer at 660 nm ($n = 3$ per group). For control tests, 30 μL of PBS solution was used instead of the test solution. The percentage of inhibition was calculated according to the following equation.

$$\text{\% Inhibition} = \frac{A_{control} - A_{sample}}{A_{control}} \times 100$$

where $A_{control}$ and A_{sample} refer to absorbance values of control and test solutions, respectively.

2.6 Antioxidant activity assay

The antioxidant activity of RosA-loaded nanofibers was determined with 1,1′-diphenyl-2-picrylhydrazyl (DPPH, Sigma Aldrich) radicals. The calibration curves and concentrations that are expected to exhibit 50% inhibition (IC_{50}) were determined for RosA in both acetone and sodium acetate buffer solution. According to calculated IC_{50} values, test solutions of nanofibers were prepared as described in Supporting Information. Then, 100 μL of each test solution was added into 1400 μL of 0.1 mM methanolic DPPH solution at room temperature. For control tests, 100 μL of blank solution (either acetone or acetate buffer) was used instead of the test solution. After keeping the mixture in dark for 1 h, the absorbance of the solution was measured using a Jenway 6300 spectrophotometer at 517 nm ($n = 3$ per group). The antioxidant activity was calculated using the following equation.

$$\text{Antioxidant activity (\%)} = \frac{A_{control} - A_{sample}}{A_{control}} \times 100$$

where $A_{control}$ and A_{sample} refer to absorbance values of control and test solutions, respectively.

2.7 Indirect cytotoxicity assay

The indirect cytotoxicity assay was performed according to ISO 10993–5 standard test method. Epithelial cells (Pasteur Institute of Iran) were cultured in Dulbecco's modified Eagle's medium (DMEM) supplemented with 10% fetal bovine serum (Gibco), 100 U/mL penicillin (Gibco), and 100 μg/mL streptomycin (Gibco) in a 5% CO_2 environment at 37°C. Extract of samples was prepared according to ISO 10993-12. About 6 cm^2 of each sample sterilized under ultraviolet radiation for 1 h was submersed in 1 mL of serum-free medium (SFM) at 37°C for 4 h. RosA solutions with concentrations of 50 and 100 μg/mL (approximately equivalent to amount of RosA released from CA/5% RosA and CA/10% RosA mats after 4 h, respectively) in SFM were also prepared. The cells were separated by trypsinization, centrifuged and seeded in wells of a 96-well tissue culture polystyrene plate at 15000 cells/well in serum-containing medium for 24 h to allow cell attachment. The cells were then starved with SFM for 24 h. Thereafter, the medium was replaced with either the RosA containing medium or extraction medium and cells were incubated for 24 h ($n = 3$ per group). Cells cultured by fresh SFM were used as the control group. Finally, the viability of cells was determined with MTT assay. After 24 h of incubation, the solution of each well was aspirated, and replaced with 100 μL/well of MTT solution (5 mg/mL MTT reagent (Sigma Aldrich) in PBS) for 4 h. The solution was then thrown away and 100 μL/well of DMSO was added for 2 h to dissolve the formazan crystals. The optical density of each well was measured with an ELISA microplate reader (Garni Medical Co., DA-3200) at 560 nm. The relative cell viability in response to each sample was expressed as a percentage of the control group (The relative cell viability of the control was defined as 100%). According to ISO 10993–5 standard test method, samples with a relative cell viability >70% of the control group were considered as biocompatible and non-cytotoxic materials.

2.8 Statistical analysis

All data are expressed as mean ± SD. One- way ANOVA followed by Tukey's post hoc test was used for multiple comparison between groups (S Plus 8.0). A value of $p < 0.05$ was considered statistically significant.

3 Results

3.1 Characterization of electrospun nanofibers

The morphology of electrospun nanofibers was visualized using SEM. SEM images of beadless electrospun neat CA, CA/5% RosA and CA/10% RosA nanofibers shown in Fig. 1 revealed no RosA aggregation on the surface of the fibers implying perfectly incorporation of RosA into nanofibers. Randomly arranged fibers of neat CA, CA/5% RosA and CA/10% RosA have average fiber diameters of 326 ± 69 nm, 314 ± 95 nm, and 331±85 nm, respectively (Table 1) which demonstrate that incorporation of RosA into fibers did not influence the fiber diameter ($p > 0.5$). Additionally there was not seen any dependency of fiber diameter on the initial amount of RosA loaded into polymer solution ($p > 0.5$) according with results previously reported for drug-loaded CA nanofibers [6, 8].

The presence of RosA in RosA-loaded nanofibers was examined by FTIR. FTIR spectra of RosA powder, and electrpspun nanofibers are shown in Fig. 2(A). For RosA powder, the bands around 1605, 1520, and 1445 cm^{-1} are due to the presence of aromatic rings indicating an aromatic ring stretching.

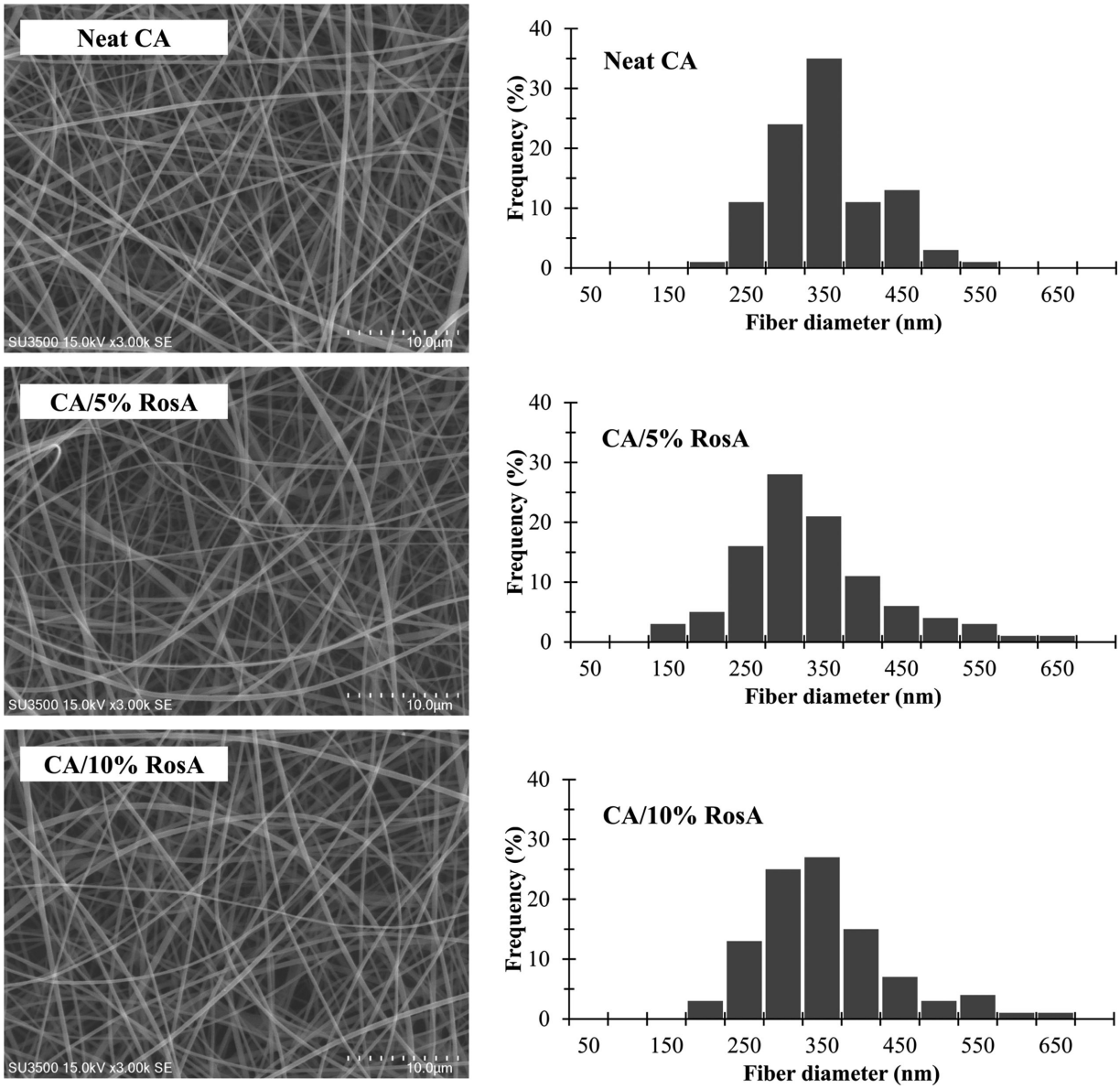

Figure 1. SEM micrographs and fiber diameter distribution of neat and RosA-loaded CA nanofibers.

Table 1. Summary of fiber diameter, and loading efficiency of different formulations, as well as diffusion constant (n) and regression coefficient (R^2) of RosA release from electrospun nanofibers

Formulation	Neat CA	CA/5% RosA	CA/10% RosA
Fiber diameter (nm)	326 ± 69	314 ± 95	331 ± 85
Initial amount of RosA loaded in 5 mg of nanofibers (μg)	-	250	500
Actual amount of RosA loaded in 5 mg of nanofibers (μg)	-	223 ± 31	422 ± 18
Loading efficiency (%)	-	89 ± 12	84 ± 4
n	-	0.372	0.437
R^2		0.97	0.99
Release mechanism	-	Fickian diffusion	Fickian diffusion

The bands around 1360 and 1180 cm^{-1} resulted from O–H and C–O stretches are evidences for phenolic groups of RosA. The characteristic band of carboxylic acid groups in the range of 1725–1700 cm^{-1} and the absorption band of an ester formation at 1750–1725 cm^{-1} are shifted to wave numbers lower than 1700 cm^{-1} in presence of aromatic structures. Therefore, the band at 1664 cm^{-1} might be due to the mentioned functional groups [18–20]. Electrospun CA nanofibers showed characteristic bands of polysaccharides including a wide stretching band of the hydroxyl groups in the range of 3700- 3050 cm^{-1} due to inter-and intramolecular bonding, the C–H methylene group stretching vibrations in the range of 3000–2800 cm^{-1}, and asymmetric and symmetric bending of methylene groups at 1435 and 1370 cm^{-1}, respectively. In addition, the band observed at 1738 cm^{-1} is due to the carbonyl stretch of the ester group of CA. The bands corresponding to asymmetric stretching of C–O–C bond of the ester group, glycosidic linkage and pyranose ring of CA are appeared around 1234, 1160, and 1049 cm^{-1}, respectively [21, 22]. Although RosA-loaded nanofibers exhibited dominant signals of CA, bands of RosA related to the ring stretching modes at 1605 and 1520 cm^{-1} are detectable confirming the presence of the RosA in the fibers. Other characteristic peaks of RosA cannot be clearly identified in spectra of RosA-loaded nanofibers due to significant overlapping with peaks of CA. By increasing the RosA loaded into nanofibers, bands assigned to hydroxyl and carbonyl bonds of CA exhibited red shifts ascertaining the formation of interactions between RosA and CA which results in obtaining the homogeneous RosA-loaded nanofibers.

DSC was performed to understand the behavior of RosA, neat and RosA-loaded CA nanofibers. The thermograms are displayed in Fig. 2(B). The DSC thermogram of RosA powder showed a sharp endothermic peak at 126°C corresponding to melting point of RosA. This endothermic peak was observed neither for CA/5% RosA nor for CA/10% RosA nanofibers. This indicates that the crystalline structure of RosA disappeared in the loaded fibers. The neat CA fibers exhibited a melting point at 236°C. The melting temperature was decreased to 227°C and 218°C, for CA/5% RosA and CA/10% RosA nanofibers, respectively. Additionally by increasing the initial drug loading, endothermic peak with lower enthalpy was seen which can be attributed to decreasing the crystalline structure of CA by increasing the RosA loaded into fibers due to uniformly dispersing the drug in the CA matrix and interrupting the hydrogen bonding among the CA chains [23].

The values of weight loss and degree of swelling of both the neat and RosA-loaded CA nanofibrous mats were evaluated. The weight loss of the neat CA, CA/5% RosA and CA/10% RosA mats shown in Fig. 3(A), was 1.7 ± 0.7%, 3.5 ± 0.7%, and 4.4 ± 1.5%, respectively and no significant differences in weight loss were observed ($p > 0.05$). The small values of weight loss resulted from the retention of the structural integrity of the neat and RosA-loaded nanofibers after submersion in the acetate buffer solution at 37°C for 24 h. As illustrated in

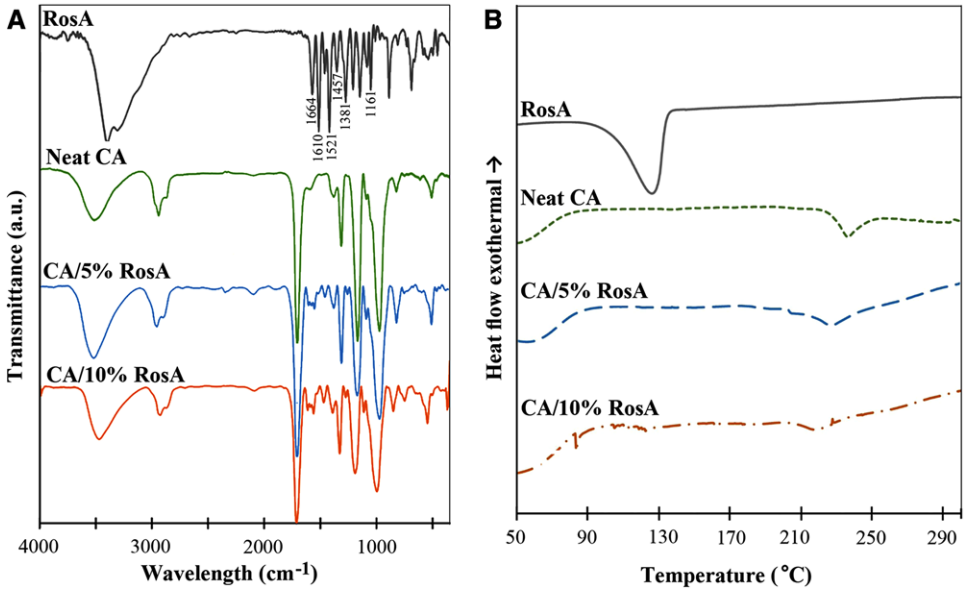

Figure 2. (A) FTIR spectra and (B) DSC thermograms of free RosA powder, neat and RosA-loaded CA nanofibers.

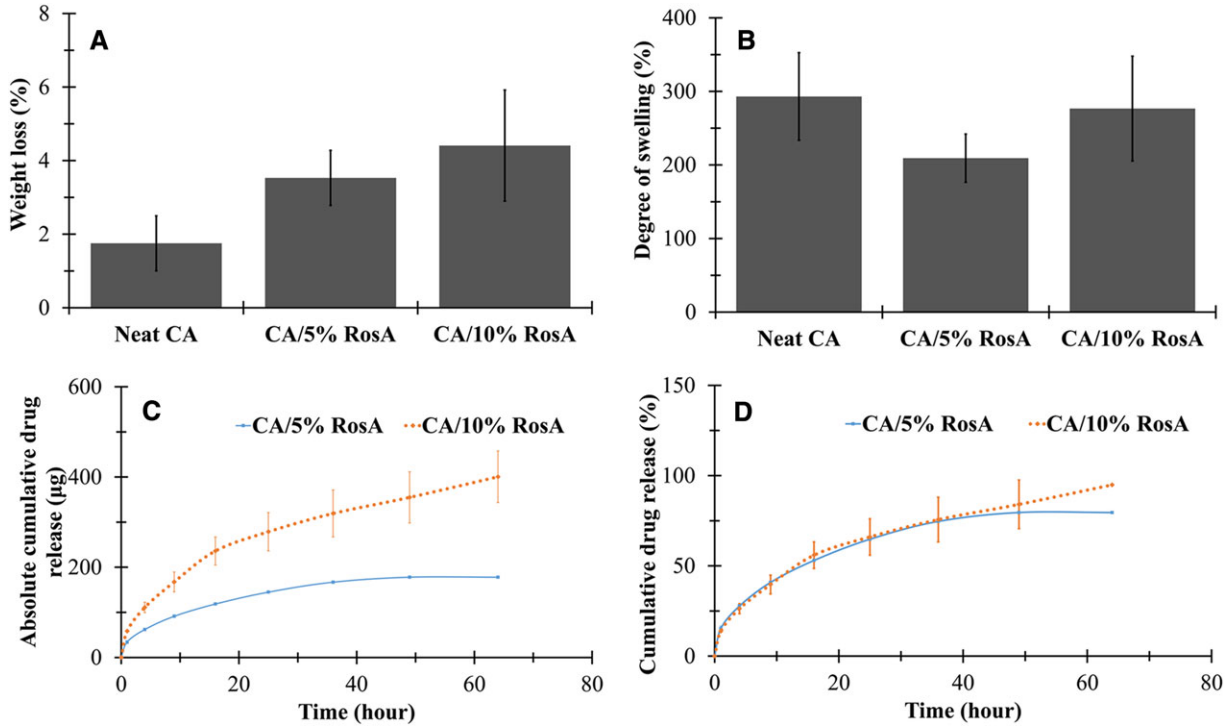

Figure 3. (A) Weight loss and (B) degree of swelling of neat and RosA-loaded CA nanofibers. (C) Cumulative absolute amount and (D) cumulative percentage of RosA released from RosA-loaded CA naofibers.

Fig. 3(B), the degree of swelling of the neat CA, CA/5% RosA and CA/10% RosA mats was 293 ± 59%, 209 ± 33%, and 277 ± 71%, respectively which did not show any significant differences ($p > 0.05$). The large amount of water absorbed in electrospun neat and RosA-loaded CA nanofibrous mats is attributed to the amount of water physically absorbed in the individual fibers and the amount of water retained by the capillary action in the inter-fibrous pores [9].

3.2 Drug loading efficiency

The values of actual amount of RosA loaded into fibers and loading efficiency are summarized in Table 1. Evidently the actual amount of RosA within drug-loaded mats was increased by increasing the initial drug loading. The loading efficiency of CA/5% RosA and CA/10% RosA mats was determined to be 89 ± 12%, and 84 ± 4%, respectively, which did not show any significant differences ($p > 0.05$) suggesting no dependency of RosA entrapment on the initial drug loading. This finding is consistent with the result reported by Suwantong et al. for CA nanofibers containing phenolic compounds [8].

3.3 In vitro RosA release behavior

The in vitro release profile of RosA from electrospun CA fibers with various RosA contents as a function of submersion time is illustrated in Fig. 3(C and D). Sustained release of RosA up to 64 h was observed for both CA/5% RosA and CA/10% RosA mats.

As expected, the maximum amount of RosA released from electrospun fibers was increased with increasing the initial RosA loading. The total amounts of RosA released from5 mg CA/5% RosA and CA/10% RosA mats were 178 ± 1 μg and 400 ± 57 μg, respectively (Fig. 3C).

The profiles related to cumulative percentage of drug release were similar for both RosA-loaded nanofibers regardless of the initial drug loading (Fig. 3D). The lack of drug aggregation on the surface of the fibers suggesting the homogeneous dispersion of RosA in the fibers resulted in relatively low initial burst release. Within the first hour, about 15 ± 1% and 14 ± 1% of RosA was released from CA/5% RosA and CA/10% RosA mats, respectively. After 64 h of incubation, the cumulative percentage of RosA released from CA/5% RosA and CA/10% RosA nanofibers reached 79 ± 1% and 95 ± 13%, respectively. However, the initial amount of RosA did not significantly affect the initial burst release as well as the drug release rate over time ($p > 0.05$).

Due to homogeneous distribution of the RosA in the nanofibers, the RosA release profile from drug-loaded nanofibrous mats was analyzed using Ritger-Peppas equation [10]. The calculated kinetic release parameters are presented in Table 1. The high correlation coefficients of the regression (R^2) confirmed that Ritger-Peppas model was acceptable to describe the mechanism of RosA release from nanofibrous mats. As implied by values of n, release from both RosA-loaded nanofibers followed Fickian diffusion mechanism irrespective of the initial drug loading.

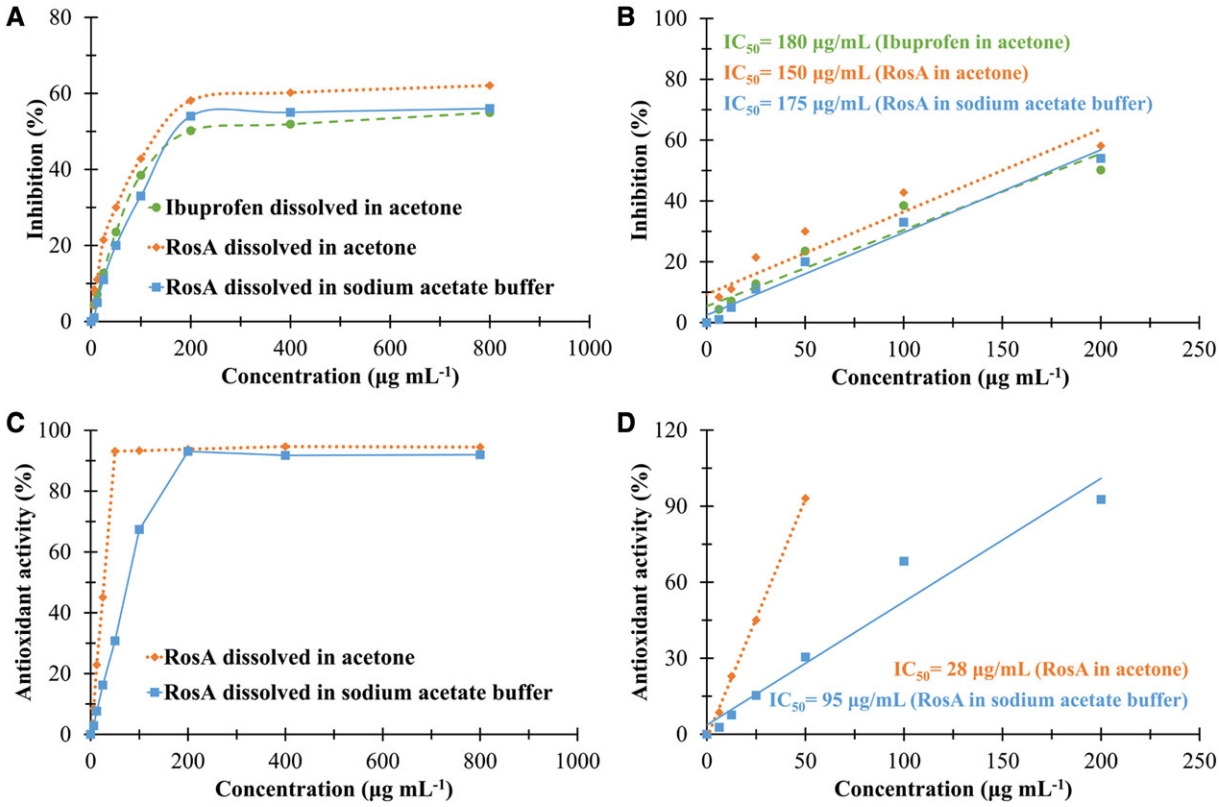

Figure 4. (A) In vitro anti-inflammatory activity of ibuprofen dissolved in acetone, and RosA dissolved in acetone and sodium acetate buffer solution at various concentrations. (B) Linear part of inhibition of protein denaturation versus concentration presenting IC_{50} values. (C) Antioxidant activity of RosA dissolved in acetone and sodium acetate buffer solution at various concentrations. (D) Linear part of antioxidant activity versus concentration presenting IC_{50} values.

3.4 In vitro anti-inflammatory activity

As evident from Fig. 4 (A-B), the IC_{50} values of ibuprofen in acetone, RosA in acetone, and RosA in acetate buffer were 180, 150, and 175 μg/mL at correlation values (R^2) of 0.92, 0.90, and 0.98, respectively. As presented in Table 2, 5 mg of CA/10% RosA nanofibers dissolved in 3 mL of acetone, exhibited inhibition of 49 $\pm$ 4%, which is comparable to inhibition activity of ibuprofen (50 $\pm$4%, $p \geq 0.05$) and significantly higher than that of CA/5% RosA nanofibers (32 $\pm$ 3%, $p < 0.05$). Similarly, RosA released from 5 mg of CA/10% RosA nanofibers into 2 mL buffer solution showed meaningfully higher activity than RosA released from CA/5% RosA nanofibers ($p < 0.05$). Additionally, the anti-inflammatory activity of RosA released from nanofibers increased as the extraction period was increased. Comparison between the activity of RosA loaded into nanofibers (Table 2) and that of free RosA (Fig. 4A and B) demonstrated that the anti-inflammatory activity of RosA did not significantly decreased by entrapment within nanofibers.

3.5 Antioxidant activity

The DPPH assay for antioxidant evaluation is based on the reduction of the free radical DPPH which is stable at room temperature in the presence of a hydrogen donating antioxidant molecule accompanied by a color change from violet to colorless [24]. The IC_{50} values of RosA in acetone and RosA in acetate buffer were found 28 and 95 μg/mL at correlation values (R^2) of 0.98 and 0.96, respectively (Fig. 4 C and D). As expected, neat CA nanofibers did not exhibit any antioxidant activity, though 5 mg of RosA/5% CA or RosA/10% CA nanofibers dissolved in 10 mL of acetone exerted antioxidant activities of 35 $\pm$ 1% and 79 $\pm$ 2% (Table 2), respectively with no significant differences compared to antioxidant activity of equivalent free RosA in acetone (Fig. 4C and D). As summarized in Table 2, the antioxidant activity of RosA released from nanofibers into buffer solution increased by extraction time ($p < 0.05$) and reached 41 $\pm$ 1% and 82 $\pm$ 1 after an extraction time of 25 h for CA/5% RosA and CA/10% RosA nanofibers, respectively. The results also indicated that antioxidant activity increased by increasing the initial RosA loading within nanofibers ($p < 0.05$).

3.6 In vitro biocompatibility

The indirect cytotoxicity assay was used to evaluate the potential of RosA-loaded nanofibrous mats to be used as transdermal patches. The relative viability of epithelial cells cultured with media containing RosA or extracts from neat and RosA-loaded

Table 2. Bioactivity of neat and RosA-loaded CA nanofibers as well as extracts from nanofibers

Formulation	Inhibition of protein denaturation (%)	Antioxidant activity (%)
Ibuprofene dissolved in acetone (200 μg/mL)	$50 \pm 4^{\sharp}$	-
RosA released from CA/5% RosA in acetone (74 ± 10 μg/mL)[a)]	$32 \pm 3^{\sharp,\ddagger}$	-
RosA released from CA/10% RosA in acetone (140 ± 6 μg/mL)[a)]	$49 \pm 4^{\ddagger}$	-
RosA released from CA/5% RosA in acetone (22 ± 3 μg/mL)[b)]	-	$35 \pm 1^{*}$
RosA released from CA/10% RosA in acetone (42 ± 2 μg/mL)[b)]	-	$79 \pm 2^{*}$
RosA released from CA/5% RosA in buffer after 4 h (31 ± 1 μg/mL)[c)]	$9 \pm 2^{\ddagger,\dagger}$	$12.0 \pm 1^{\ddagger,\dagger}$
RosA released from CA/10% RosA in buffer after 4 h (55 ± 6 μg/mL)[c)]	$18 \pm 3^{\ddagger,\S}$	$34.0 \pm 1^{\ddagger,\S}$
RosA released from CA/5% RosA in buffer after 25 h (72 ± 1 μg/mL)[c)]	$20 \pm 2^{\sharp,\dagger}$	$41 \pm 1^{\sharp,\dagger}$
RosA released from CA/10% RosA in buffer after 25 h (139 ± 21 μg/mL)[c)]	$43 \pm 3^{\sharp,\S}$	$82 \pm 1^{\sharp,\S}$

[a)] RosA released from 5 mg nanofibers dissolved in 3 mL of acetone.
[b)] RosA released from 5 mg nanofibers dissolved in 10 mL of acetone.
[c)] RosA released from 5 mg nanofibers in 2 mL of sodium acetate buffer solution.
Bioactivity of neat CA and its extracts were negligible. ♯, ‡ *,♯, ♯,†,§ indicate significant differences between corresponding values at $p < 0.05$.

nanofibers is illustrated in Fig. 5. Although significant differences between relative viability of cells cultured in presence of media containing RosA and extraction media were observed, clearly, all the samples showed relative cell viability greater than 70% of the control group indicating low toxic effect of RosA and electrospun mats on cells.

4 Discussion

The poor bioavailability associated with low solubility of drugs is one of the most challenging aspects of formulation development.

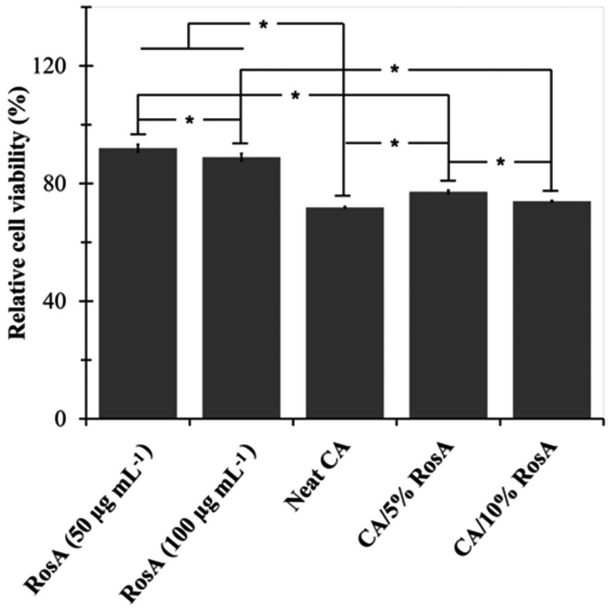

Figure 5. Relative cell viability of epithelial cells cultured with RosA containing media and extraction media from neat and RosA-loaded CA nanofibers (The relative cell viability of the control was defined as 100%). ∗ indicates significant differences.

Solid dispersion is the most appropriate method to improve the solubility and hence the bioavailability of a poorly water- soluble drug [25,26]. Electrospinning is an interesting technique in generating drug delivery systems due to its ability to combine solid dispersion and controlled release approaches [27,28]. Additionally, electrospun fibers with their high surface area to volume ratio and ability to embed a drug through dissolution or dispersion in the polymer solution can result in a high drug loading and a sustained drug delivery [29]. Electrospun nanofibers are also used as the TDDSs which are designed to facilitate the delivery of target drugs into the body through the skin [30]. The TDDSs containing NSAIDs are now being used for pain management [2]. The NSAIDs are among the most commonly used medication of inflammatory diseases to relieve the pain. NSAIDs inhibit the cyclooxygenase (COX) enzyme which catalyzes the conversion of arachidonic acid to prostaglandins and thromboxane. Due to the significant side effects of the most common NSAID medications, there is a great interest in natural compounds to reduce pain and inflammation. Natural anti-inflammatory phytochemicals inhibit not only the COX pathway, but also the nuclear factor-κB (NF-κB) inflammatory pathway [31]. Naturally derived anti-inflammatory compounds such as curcumin [8, 32], capsaicin [33, 34], ursolic acid [35] and gingerol [23] were successfully incorporated into electrospun nanofibers in order to develop transdermal patches.

Rosmarinic acid inhibits the expression of important inflammatory mediators including intercellular adhesion molecule-1 (ICAM-1), vascular cell adhesion molecule-1 (VCAM-1), keratinocyte chemo-attractant (KC), macrophage inflammatory protein-2 (MIP-2), COX and lipoxygenase (LOX) [36–39] and complement activation [36]. The gene expression of these mediators is regulated via NF-κB pathway. Rosmarinic acid as a phenolic compound is able to downregulate the NF-κB pathway [37]. In addition, reactive oxygen species play central roles as mediators in physiopathology process of inflammation [40, 41] and contribute to tissue injuries caused by inflammation [41], thus the free radical scavenging potential of RosA can assist its anti-inflammatory properties [36].

Although incorporation of RosA in micro/nanoparticles for biomedical and cosmetic applications were recently reported

by many researchers [5, 19, 20, 42–47], this is the preliminary attempt to entrap RosA within a nanofibrous matrix and to study the potential of RosA-loaded nanofibers as a drug delivery system with anti-inflammatory and antioxidant properties.

Neat and RosA-loaded CA nanofibers with diameters around 300–400 nm (Fig. 1 and Table 1) providing a large surface area to volume ratio are promising structure for a high drug loading and a sustained drug delivery.

FTIR spectroscopy (Fig. 2A) proving the formation of hydrogen bonds between CA and RosA corroborates good compatibility of RosA with CA. Existence of the drug crystal in a transdermal patch restricts the uptake of drug through the skin decreasing the bioavailability of the drug. Therefore, inhibition of the drug recrystallization is essential in order to maintain the efficiency and quality of the transdermal patch. The fast evaporation of solvent during electrospinning process results in freezing drug molecules in nanofibrous matrix inhibiting the formation of drug crystals [11]. As illustrated in Fig. 2B, no crystalline drug was present at nanofibrous CA/5% RosA and CA/10% RosA mats demonstrating the dispersion of RosA molecules in an amorphous state in CA nanofibers.

Since CA is soluble in glacial acetic acid, it is expected that electrospun CA fibers are partially dissolved in the acetate buffer solution. However, the crystalline structure of both the neat and RosA-loaded CA nanofibrous mats inferred from their melting endotherm peaks (Fig. 2B) would limit the accessibility of the acetate buffer and thus the weight loss. However, decreasing the crystallinity of polymer carrier resulting from increasing the initial drug loading increased the weight loss, albeit this increase was not statistically meaningful (Figure 3A).

Association of RosA with CA matrix by strong linkages, homogeneous distribution of the drug within RosA-loaded solutions due to the solubility of the RosA in acetone/DMAc and the presence of drug in an amorphous state within nanofibers play complementary roles in successfully entrapment of the drug inside the nanofibers with a high loading efficiency (Table 1), low burst release, prolonged drug release, and releasing a large percentage of the drug [10] (Fig. 3C and D). The results of this study revealed the great merit of CA nanofibers as RosA delivery patches compared to the previously reported polymer-based RosA delivery systems. The loading efficiency of 40–60% and the fast initial release of around 90–100% of RosA in 30–45 min that were reported for chitosan micro/nanoparticle-based RosA delivery systems prepared by ionic gelation or spray drying might be due to association of RosA with particles on their surfaces by weak linkages [20, 45, 47].

According to Ritger-Peppas model, the release of RosA from nanofibers is controlled by Fickian diffusion release mechanism (Table 1). Diffusion of the drug from a polymeric matrix corresponds to two mechanisms including drug diffusion out of the matrix, and drug diffusion due to matrix degradation [12]. Since semi-crystallinity of polymeric CA carriers restrains degradation in acetate buffer, RosA release is predominantly attributed to the diffusion or permeation of the drug through CA nanofibers.

For a drug delivery system, retention of bioactivity of the drug is also of great importance. Therefore to ensure that solvent and electrical potential used in the fabrication process did not cause any destruction in RosA properties, the anti-inflammatory and antioxidant activities of RosA-loaded nanofibers were studied and compared to those of free RosA.

Through protein denaturation induced by a strong acid or base, a concentrated inorganic salt, or heat, proteins lose their tertiary and secondary structures and biological functions [48]. Protein denaturation is a well-documented cause of inflammation. The compounds inhibiting the denaturation of proteins in vitro might be used as anti-inflammatory agents. Therefore, BSA denaturation method is an appropriate assay for the evaluation of anti-inflammatory properties of a compound in vitro. BSA denaturation caused by heating is followed by expression of antigens associated with type III hypersensitive reaction which in turn is related to chronic inflammatory diseases [49]. In the present work, RosA and RosA-loaded nanofibrous mats showed anti-inflammatory activity comparable to ibuprofen, a NSAID standard drug, by inhibition of the BSA denaturation (Fig. 4A and B and Table 2). Therefore, as anticipated, electrospinning process does not have any adverse impact on RosA bioactivity. In vitro assessment of anti-inflammatory activity can be supplemented with membrane stabilization assay and heat induced hemolysis test [48].

The IC_{50} value is an indicator of antioxidant capacity of a product. RosA used in this study exhibited IC_{50} values within the range of 1 to 50 μg/mL and 50 to 100 μg/mL corroborating very high and high antioxidant activity [50] of RosA dissolved in acetone and acetate buffer, respectively. RosA is an ester of caffeic acid with 3,4-dihydroxyphenyl lactic acid. Its four phenolic hydrogen specially two electroactive catechol moieties can neutralize free radicals by an electron/proton donor mechanism [4, 51]. RosA loaded into nanofibers could maintain its antioxidant activity without experiencing any deterioration after being subjected to a high electrical potential (Fig. 4C and D and Table 2).

To simulate the clinical use conditions so as to evaluate the potential toxicological hazard of RosA, neat and RosA-loaded nanofibers, the extract of samples was used. The acceptable values of relative cell viability confirmed the negligible hazard potential of neat and RosA-loaded nanofibrous mats (Figure 5). While the biocompatibility of CA nanofibers was also revealed by other researchers [8, 23], the results proved the potential of RosA to improve cell viability.

The overall results of this study demonstrate that electrospinning can be successfully employed to fabricate RosA-loaded nanofibers with high loading efficiency. Additionally, RosA loaded into nanofibers retained its bioactivity and biocompatibility while it could be sustained release over a period of 64 h irrespective of the initial drug loading. Therefore, RosA-loaded CA nanofibers are potential candidate for developing anti-inflammatory and antioxidant transdermal patches.

Practical application

Rosmarinic acid, a phytochemical with non-steroidal anti-inflammatory and antioxidant activities was loaded in CA nanofibrous mats using electrospinning process to improve its bioavailability and biostability. The electrospun nanofibers exhibited smooth morphology with uniform size distribution. Rosmarinic acid interacting with CA was molecularly dispersed within the polymer carrier in an amorphous state allowing a high loading efficiency, a low burst release and a sustained release of RosA for a period of 64 h. Although a decrease in crystallinity of CA nanofibers was observed by increasing the RosA content within nanofibers, RosA-loaded CA nanofibers exhibited a semi-crystalline nature which restricted degradation of nanofibers in acetate buffer solution resulting in predominance of Fickian diffusion mechanism. Additionally, RosA-loaded nanofibers exhibited anti-inflammatory, antioxidant and biocompatibility properties. Taking these promising findings into account, the validation of electrospun RosA-loaded nanofibers as a drug delivery system for pain management can be confirmed.

This work was supported by Shahid Beheshti University G.C.(grant number 600/1175). The author gratefully acknowledges Bioproducts and Biosystems Laboratories of Shahid Beheshti University, Zirab Campus for technical support and Alborz Bulk Pharmaceutical Co. for kindly providing "ibuprofen" used in this research.

The authors have declared no conflict of interest.

5 References

[1] Wokovich, A. M., Prodduturi, S., Doub, W. H., Hussain, A. S., et al., Transdermal drug delivery system (TDDS) adhesion as a critical safety, efficacy and quality attribute. *Eur J Pharm Biopharm.* 2006, *64*, 1–8.

[2] Bajaj, S., Whiteman, A., Brandner, B., Transdermal drug delivery in pain management. *Continuing Education in Anaesthesia, Critical Care & Pain* 2011, *11*, 39–43.

[3] Takano, H., Osakabe, N., Sanbongi, C., Yanagisawa, R. et al., Extract of Perilla frutescens enriched for rosmarinic acid, a polyphenolic phytochemical, inhibits seasonal allergic rhinoconjunctivitis in humans. *Exp Biol Med (Maywood)* 2004, *229*, 247–254.

[4] Amoah, S. K., Sandjo, L. P., Kratz, J. M., Biavatti, M. W., Rosmarinic acid-pharmaceutical and clinical aspects. *Planta Med.* 2016, *82*, 388–406.

[5] Yücel, Ç., Şeker-Karatoprak, G., Development and evaluation of the antioxidant activity of liposomes and nanospheres containing rosmarinic acid. *Farmacia* 2017, *65*, 40–45.

[6] Taepaiboon, P., Rungsardthong, U., Supaphol, P., Vitamin-loaded electrospun cellulose acetate nanofiber mats as transdermal and dermal therapeutic agents of vitamin A acid and vitamin E. *Eur J Pharm Biopharm.* 2007, *67*, 387–397.

[7] Kontogiannopoulos, K. N., Assimopoulou, A. N., Tsivintzelis, I., Panayiotou, C., et al., Electrospun fiber mats containing shikonin and derivatives with potential biomedical applications. *Int J Pharm.* 2011, *409*, 216–228.

[8] Suwantong, O., Opanasopit, P., Ruktanonchai, U., Supaphol, P., Electrospun cellulose acetate fiber mats containing curcumin and release characteristic of the herbal substance. *Polymer* 2007, *48*, 7546–7557.

[9] Tungprapa, S., Jangchud, I., Supaphol, P., Release characteristics of four model drugs from drug-loaded electrospun cellulose acetate fiber mats. *Polymer* 2007, *48*, 5030–5041.

[10] Yu, D. G., Li, X. Y., Wang, X., Chian, W. et al., Zero-order drug release cellulose acetate nanofibers prepared using coaxial electrospinning. *Cellulose* 2013, *20*, 379–389.

[11] Shi, Y., Wei, Z., Zhao, H., Liu, T. et al., Electrospinning of ibuprofen-loaded composite nanofibers for improving the performances of transdermal patches. *J. Nanosci Nanotechnol.* 2013, *13*, 3855–3863.

[12] Jannesari, M., Varshosaz, J., Morshed, M., Zamani, M., Composite poly (vinyl alcohol)/poly (vinyl acetate) electrospun nanofibrous mats as a novel wound dressing matrix for controlled release of drugs. *Int J Nanomedicine* 2011; *6*: 993–1003.

[13] Zhang, Y., Huo, M., Zhou, J., Zou, A. et al., DDSolver: an add-in program for modeling and comparison of drug sissolution profiles. *AAPS J.* 2010, *12*, 263–271.

[14] Serra, L., Doménech, J., Peppas, N. A., Drug transport mechanisms and release kinetics from molecularly designed poly (acrylic acid-g-ethylene glycol) hydrogels. *Biomaterials.* 2006, *27*, 5440–5451.

[15] Korsmeyer, R. W., Gurny, R., Doelker, E., Buri, P., et al., Mechanisms of solute release from porous hydrophilic polymers. *Int J Pharm.* 1983, *15*, 25–35.

[16] Mendes, A. C., Gorzelanny, C., Halter, N., Schneider, S. W., et al., Hybrid electrospun chitosan-phospholipids nanofibers for transdermal drug delivery. *Int J Pharm.* 2016, *510*, 48–56.

[17] Mizushima, Y., Kobayashi, M., Interaction of anti-inflammatory drugs with serum proteins, especially with some biologically active proteins. *J Pharm Pharmacol.* 1968, *20*, 169–173.

[18] Stehfest, K., Boese, M., Kerns, G., Piry, A., et al., Fourier transform infrared spectroscopy as a new tool to determine rosmarinic acid in situ. *J Plant Physiol.* 2004, *161*, 151–156.

[19] Campos, D. A., Madureira, A. R., Gomes, A. M., Sarmento, B., et al., Optimization of the production of solid Witepsol nanoparticles loaded with rosmarinic acid. *Colloids Surf B Biointerfaces.* 2014, *115*, 109–117.

[20] da Silva, S. B., Amorim, M., Fonte, P., Madureira, R. et al., Natural extracts into chitosan nanocarriers for rosmarinic acid drug delivery. *Pharm Biol.* 2015, *53*, 642–652.

[21] Vallejos, M. E., Peresin, M. S., Rojas, O. J., All-cellulose composite fibers obtained by electrospinning dispersions of cellulose acetate and cellulose nanocrystals. *J Polym Environ.* 2012, *20*, 1075–1083.

[22] Vatankhah, E., Prabhakaran, M. P., Jin, G., Ghasemi Mobarakeh, L., et al., Development of nanofibrous cellulose acetate/gelatin skin substitutes for variety wound treatment applications. *J Biomater Appl.* 2013, *28*, 909–921.

[23] Chantarodsakun, T., Vongsetskul, T., Jangpatarapongsa, K., Tuchinda, P. et al., [6]-Gingerol-loaded cellulose acetate

electrospun fibers as a topical carrier for controlled release. *Polym Bull.* 2014, *71*, 3163–3176.
[24] Garcia, E. J., Oldoni, T. L. C., Alencar, S. M., Reis, A. et al., Antioxidant activity by DPPH assay of potential solutions to be applied on bleached teeth. *Braz Dent J.* 2012, *23*, 22–27.
[25] Verreck, G., Chun, I., Peeters, J., Rosenblatt, J., et al., Preparation and characterization of nanofibers containing amorphous drug dispersions generated by electrostatic spinning. *Pharm Res.* 2003, *20*, 810–817.
[26] Yu, D. G., Williams, G. R., Wang, X., Yang, J. H. et al., Polymer-based nanoparticulate solid dispersions prepared by a modified electrospraying process. *J Biomed Sci Eng.* 2011, *4*, 741–749.
[27] Chakraborty, S., Liao, I-C., Adler, A., Leong, K. W., Electrohydrodynamics: a facile technique to fabricate drug delivery systems. *Adv Drug Deliv Rev.* 2009, *61*, 1043–1054.
[28] Paaver, U., Heinämäki, J., Laidmäe, I., Lust, A. et al., Electrospun nanofibers as a potential controlled-release solid dispersion system for poorly water-soluble drugs. *Int J Pharm.* 2015, *479*, 252–260.
[29] Ball, C., Woodrow, K. A., Electrospun solid dispersions of maraviroc for rapid intravaginal preexposure prophylaxis of HIV. *Antimicrob Agents Chemother.* 2014, *58*, 4855–4865.
[30] Zamani, M., Prabhakaran, M. P., Ramakrishna, S., Advances in drug delivery via electrospun and electrosprayed nanomaterials. *Int J Nanomedicine.* 2013, *8*, 2997–3017.
[31] Maroon, J. C., Bost, J. W., Maroon, A., Natural anti-inflammatory agents for pain relief. *Surg Neurol Int.* 2010, *1*, 80.
[32] Merrell, J. G., McLaughlin, S. W., Tie, L., Laurencin, C. T. et al., Curcumin-loaded poly (ε-caprolactone) nanofibres: diabetic wound dressing with anti-oxidant and anti-inflammatory properties. *Clin Exp Pharmacol Physiol.* 2009, *36*, 1149–1156.
[33] Ngawhirunpat, T., Rojanarata, T., Panomsuk, S., Opanasopit, P., Fabrication of capsaicin loaded polyvinyl alcohol electrospun nanofibers. *Adv Mat Res.* 2011, *338*, 42–45.
[34] Opanasopit, P., Sila-on, W., Rojanarata, T., Ngawhirunpat, T., Fabrication and properties of capsicum extract-loaded PVA and CA nanofiber patches. *Pharm Dev Technol.* 2013, *18*, 1140–1147.
[35] Huang, L.-y., Yu, D.-g., Zhu, L. M., Branford-White, C. J., et al., Preparation of fast-dissolving ursolic acid nanofiber membrances using electrospinning, In: *Bioinformatics and Biomedical Engineering,(iCBBE) 2011 5th International Conference on* 2011, pp.1-4. IEEE.
[36] Youn, J., Lee, K. H., Won, J., Huh, S. J. et al., Beneficial effects of rosmarinic acid on suppression of collagen induced arthritis. *J Rheumatol.* 2003, *30*, 1203–1207.
[37] Osakabe, N., Yasuda, A., Natsume, M., Yoshikawa, T., Rosmarinic acid inhibits epidermal inflammatory responses: anticarcinogenic effect of Perilla frutescens extract in the murine two-stage skin model. *Carcinogenesis.* 2004, *25*, 549–557.
[38] Lee, J., Jung, E., Kim, Y., Lee, J. et al., Rosmarinic acid as a downstream inhibitor of IKK-β in TNF-α-induced upregulation of CCL11 and CCR3. *Br J Pharmacol.* 2006, *148*, 366–375.
[39] Kim, H. K., Lee, J. J., Lee, J. S., Park, Y. M., et al., Rosmarinic acid down-regulates the LPS-induced production of monocyte chemoattractant protein-1 (MCP-1) and macrophage inflammatory protein-1alpha (MIP-1alpha) via the MAPK pathway in bone-marrow derived dendritic cells. *Mol Cells.* 2008, *26*, 583–589.
[40] Priya, T. T., Sabu, M. C., Jolly, C. I., Free radical scavenging and anti-inflammatory properties of Lagerstroemia speciosa (L). *Inflammopharmacology.* 2008, *16*, 182–187.
[41] Rocha, J., Eduardo-Figueira, M., Barateiro, A., Fernandes, A. et al., Anti-inflammatory effect of rosmarinic acid and an extract of rosmarinus officinalis in rat models of local and systemic inflammation. *Basic Clin Pharmacol Toxicol.* 2015, *116*, 398–413.
[42] Kim, H-J., Kim, T-H., Kang, K-C., Pyo, H-B., et al., Microencapsulation of rosmarinic acid using polycaprolactone and various surfactants. *Int J Cosmet Sci.* 2010, *32*, 185–191.
[43] Budhiraja, A. and Dhingra, G., Development and characterization of a novel antiacne niosomal gel of rosmarinic acid. *Drug Deliv.* 2015, *22*, 723–730.
[44] Bhatt, R., Singh, D., Prakash, A., Mishra, N., Development, characterization and nasal delivery of rosmarinic acid-loaded solid lipid nanoparticles for the effective management of Huntington's disease. *Drug deliv.* 2015, *22*, 931–939.
[45] Casanova, F., Estevinho, B. N., Santos, L., Preliminary studies of rosmarinic acid microencapsulation with chitosan and modified chitosan for topical delivery. *Powder Technol.* 2016, *297*, 44–49.
[46] Rijo, P., Matias, D., Fernandes, A. S., Simões, M. F. et al., Antimicrobial plant extracts encapsulated into polymeric beads for potential application on the skin. *Polymers.* 2014, *6*, 479–490.
[47] da Silva, S. B., Ferreira, D., Pintado, M., Bruno, S., Chitosan-based nanoparticles for rosmarinic acid ocular delivery-In vitro tests. *Int J Biol Macromol.* 2016, *84*, 112–120.
[48] Leelaprakash G., Dass S. M., In vitro anti-inflammatory activity of methanol extract of Enicostemma axillare. *Int. J. Drug Dev. Res.* 2011, *3*, 189–196.
[49] Elisha, I. L., Dzoyem, J-P, McGaw, L. J., Botha, F. S., et al., The anti-arthritic, anti-inflammatory, antioxidant activity and relationships with total phenolics and total flavonoids of nine South African plants used traditionally to treat arthritis. *BMC Complement Altern Med.* 2016, *16*, 307.
[50] Sriyanti, I., Edikresnha, D., Rahma, A., Munir, M. M. et al., Correlation between structures and antioxidant activities of polyvinylpyrrolidone/garcinia mangostana L. extract composite nanofiber mats prepared using electrospinning. *J Nanomater.* 2017, *2017*, 1–10.
[51] de Souza Gil, E., Adrian Enache, T. and Maria Oliveira-Brett A., Redox behaviour of verbascoside and rosmarinic acid. *Comb Chem High T Scr.* 2013, *16*, 92–97.